

# Combined effects of particle shape and strain rate on the ring shear response of granular soil

Subham Chowdhury<sup>1</sup> and Arghya Das<sup>1,\*</sup>

<sup>1</sup>Department of Civil Engineering, Indian Institute of Technology Kanpur, Kalyanpur, Uttar Pradesh – 208016, India

**Abstract.** This study aims to visualize the combined effect of shape and strain rate on the mechanical response of monodisperse granular materials through 3D DEM ring shear tests. One part of the simulations implements contact-scale rolling resistance friction (RR friction) parameters to mimic particle angularity, and the other part takes idealized spherical particles, and further subjecting both to varying normal stress and shear strain-rates. Considering both simulation schemes, lower strain-rate accentuates material stiffness along with increased contraction of the specimen. Conversely, higher strain-rate promotes delayed contraction along with higher deviatoric strength and reduced stiffness. Specimen having particle scale rolling friction gives higher peak and residual strength along with shift in critical state regime compared to idealized spherical specimens. Further, ensemble-scale porosity and co-ordination number has been investigated to provide a micro-scale perspective on the responses.

## 1 Introduction

Natural geomaterials, besides being exposed to continuous monotonic loading scenarios, also get affected by sudden strain-rate change (e.g., earthquake loading and dynamic loading due to trail wheel loads) [1]. Typically, granular soils exhibit non-isotach behaviour with temporary offshoots in macro-scale responses under sudden strain rate shifts. However, strain rate shows explicit dependency on the crushability aspects of the granular ensemble – grain fragmentation, rather than grain re-orientation, makes granular soil more prone to rate dependency [1]. Flow-based geotechnical hazards, e.g., landslides and avalanches, are characterized by progressive deformation of geomaterials, and thus, studying flow deformation of granular soil under evolving strain rate attains both relevance and significance. Conventional element scale tests like direct shear and triaxial tests carry the disadvantage of allowing a limited ambit of deformation, and extrapolating these data for dynamic conditions may lead to misinterpretation since shear stress evolves under varying strain rates. However, such a drawback is surpassed by ring shear tests [2], which theoretically allow for an infinite amount of shear deformation of the sample. One of the crucial parameters guiding the emergent macroscopic behaviour (viz. strain-rate dependency) of bulk material is the shape of the constituting particles. However, modelling realistic particle shapes in DEM is computationally intensive, so modified contact models have been developed that mimic the degree of interlocking and do away with the intensive

computational requirement when using realistic synthetic particles. The current study aims to implement a contact rolling-resistance friction parameter (mimicking particle interlocking) within a monodisperse assembly of spherical particles and compare the macro-scale response with an idealized monodisperse assembly of pure spheres. The specimens have been subjected to 3D numerical ring shear tests under varying strain-rate scenarios to investigate the combined effect of particle shape and strain rate on the macro-mechanical responses.

## 2 Numerical modelling frameworks

### 2.1 Rolling Resistance Friction mechanics

Since modelling realistic particle shapes in 3D DEM framework has computational consequences, a more efficient contact model has been developed which helps

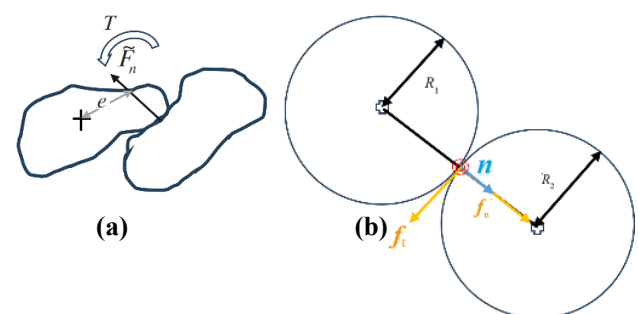


**Figure 1.** (a) Contact between two realistic particles (after [3]) (b) Rolling resistance contact model

\* Corresponding author: [arghya@iitk.ac.in](mailto:arghya@iitk.ac.in)

to introduce ‘role of shape’ in an idealized spherical ensemble of granular materials [3]. In non-spherical case [Fig. 1(a)], the contact normal force vector mostly bypasses the centroid of the particle, generating a small amount of eccentricity  $e$ . The eccentricity creates a torque  $T_e$  of magnitude:

$$|T_e| = e|\tilde{F}_n| \quad (1)$$

which resists rotational perturbation. This torque should be comparable in magnitude to any ‘rolling resistance’ defined by a rolling resistance specific contact model where a resisting moment (torque  $\tilde{T}_r$ ) proportional to the normal contact force acts in a direction opposite to the rolling direction [Fig 1(b)].

$$|\tilde{T}_r| = -\mu_r R_r f_n \frac{\omega_{rel}}{|\omega_{rel}|} \quad (2)$$

where  $\mu_r$  is the coefficient of rolling friction,  $f_n$  is the contact normal force,  $\omega_{rel}$  is the relative angular velocity of the two particles in contact, and  $R_r$  is the effective rolling radius of the contact, given by:

$$R_r = \frac{R_1 R_2}{R_1 + R_2} \quad (3)$$

## 2.2 Sample generation, Contact model implementation and numerical shearing

The current ambit of simulations presents series of ring shear tests being conducted on two different monodisperse granular ensemble of spherical particles in commercial 3D DEM software Particle Fluid Code [PFC-5, Itasca]. The diameter of the generated spheres is 3 mm and density of 2600 kg/m<sup>3</sup>. At the first stage of simulation, a cloud of 12880 particles have been generated, which is allowed to freely fall in an annular setup, of outer diameter 150 mm, inner diameter 50 mm and height of 25 mm. The particles are initially subjected to a linear contact model and allowed to fall under gravity. After proper settlement, the top annular plate is brought on the surface of the specimen through a velocity-controlled scheme, and the erstwhile contact model is replaced by rolling resistance linear contact model. Both the top and bottom consists of 18 discrete flanges of height 4 mm, to provide the shearing torque on the specimen. The synthetic sample, now having significant particle overlaps, is then equilibrated in the order of 10<sup>-5</sup> by switching off the gravity. The initial porosity of the sample stands at 53 % [Fig. 2]. Two different samples are prepared: one having the rolling resistance (RR friction) coefficient (mimicking angular particles) and the other devoid of it (representing idealized spherical particles). The DEM parameters

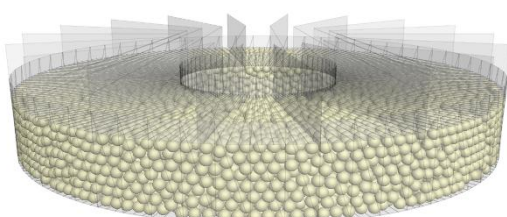
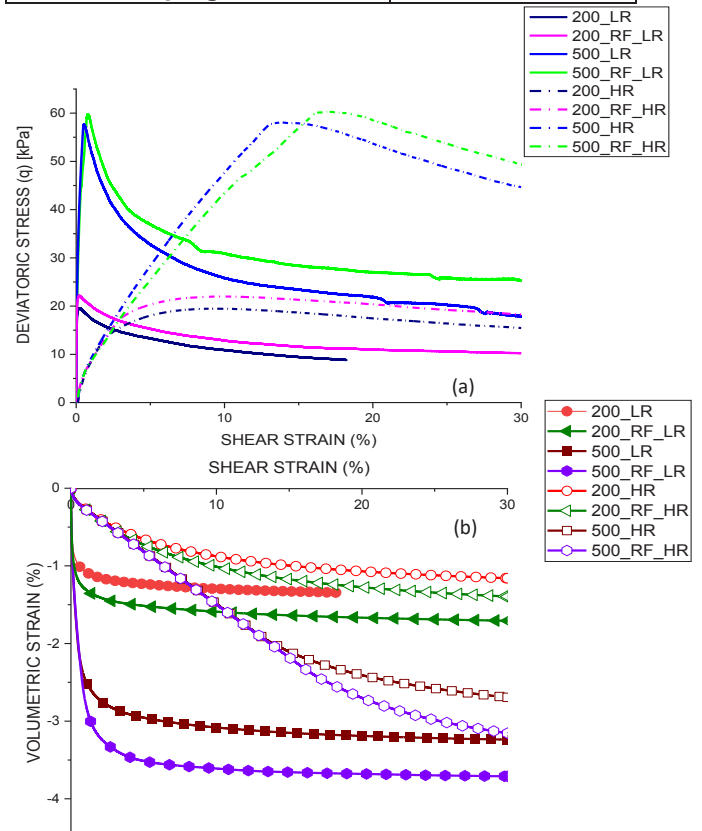


Figure 2. Numerical Ring Shear setup

implemented in the simulations for have been adopted from Alam et al.,[3] and presented in a tabular format [Table 1]. Normal stress is implemented on the top wall through servo-controlled mechanism, and maintained throughout the shearing process. Next, shear on the specimen is provided by rotating the bottom platen and its adjoining flanges to provide a shearing force to the specimen, while position of all the adjoining facets in top platen, the inner and outer circular walls have been kept fixed. Two different confinement (200 kPa and 500 kPa) and two different shear strain – rate (5.28 deg – sec<sup>-1</sup> (LR) and 52.8 deg sec<sup>-1</sup> (HR)) is implemented in the simulations. The inertial number of the system clocked in the order of 10<sup>-6</sup>, ensuring quasistatic condition.

Table 1. DEM parameters (after Alam et al.,[3]) [Note: b-b – ball-ball; b-w – ball-wall]

PARAMETERS	Values
<b>Normal Stiffness</b>	b-b: 6.3e4 N/m
	b-w: 6.42e5 N/m
<b>Shear Stiffness</b>	b-b: 6e4 N/m
	b-w: 4.23e5 N/m
<b>Normal to Shear stiffness ratio</b>	1.5
<b>Effective Modulus</b>	b-b: 1.8e9 N/m <sup>2</sup>
	b-w: 2e10 N/m <sup>2</sup>
<b>Coulomb friction coefficient</b>	b-b: 0.6
	b-w: 0.0
<b>RR friction coefficient</b>	b-b: 0.35
	b-w: 0.0
<b>Critical Normal and Shear damping ratio</b>	b-b: 0.7
	b-w: 0.0



**Figure 3.** Deviatoric stress – Shear Strain – Volumetric Strain response under 200 and 500 kPa normal stress [Nomenclature: LR/HR – Low rate/High rate; RF-presence of RR friction]

### 3 Results and discussions

#### 3.1 Deviatoric Stress-Shear Strain-Volumetric deformation response

Stress, being a continuum parameter, cannot be measured directly since the specimen is discrete, and so an averaged stress response for the entire specimen volume is obtained, given by Christoffersen et al.,[4]:

$$\sigma_{ij} = -\frac{1}{V} \sum_{N_c} F^c \otimes L^c \quad (4)$$

where  $N_c$  is the number of contacts present in the domain of volume  $V$ ,  $F^c$  is the contact force vector,  $L^c$  is the branch vector joining the centroids of the two particles in contact,  $\otimes$  denotes dyadic product, and compressive stress is negative by convention. However, stress tensor in the specimen changes with the change in direction of co-ordinate system, so the second invariant of deviator stress  $J_2$  is computed as follows:

$$J_2 = \frac{1}{6} [(\sigma_{yy} - \sigma_{zz})^2 + (\sigma_{xx} - \sigma_{yy})^2 + (\sigma_{zz} - \sigma_{xx})^2 + \tau_{xy}^2 + \tau_{yz}^2 + \tau_{zx}^2] \quad (5)$$

Finally, the distortional or deviatoric stress  $q$ , is:

$$q = (3J_2)^{1/2} \quad (6)$$

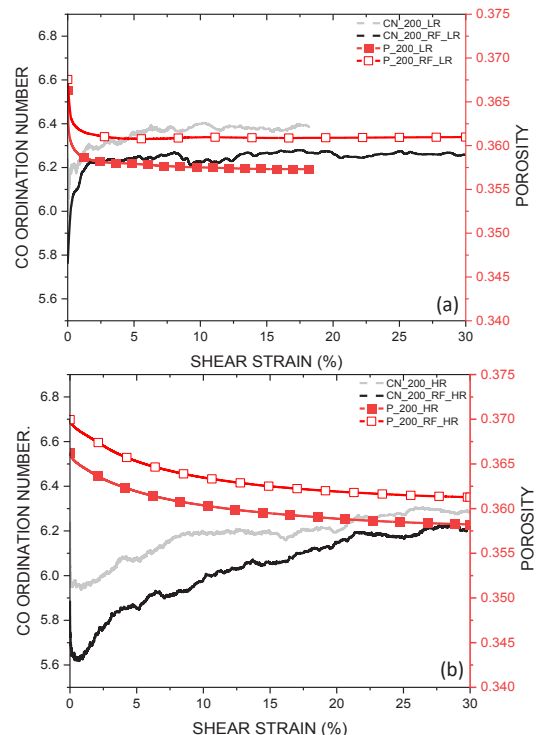
The macroscopic stress-strain-volumetric deformation response of the specimens under the 2-fold environmental constraint of strain rate and shape (incorporated through the presence of RR friction) is obtained and presented in Fig. 3 (a-b). From Fig. 3(a), the deviatoric stress-shear strain plots shows a noticeable change in macro-level response upon a change in shear strain rate from low to high. For both 200 kPa and 500 kPa normal confinement, it can be observed that the presence of rolling resistance friction (RR friction) shifts the peak strength response to a higher value when compared with the idealized spherical specimen. Further, a concurrent shift in the residual strength regime towards a higher degree, for both the confinements, in the presence of RR friction indicates the critical state behaviour is somewhat influenced due to the presence of RR friction. Though for the same confinements, due to a shift in strain rate, there has been no noticeable change in the peak response; however, the stiffness response is markedly different. The low-rate response gives significantly high stiffness (attaining peak deviatoric stress at nearly 1% shear strain) accompanied by sharp stress drop in the residual regime (mimicking brittle behaviour), and the high-rate response shows significant shift in stiffness along with a gradual stress build-up up till attaining peak strength (indicative of ductile behaviour). In high strain-rate scenarios, additional resistance in the form of inertial forces from the bulk specimen mass and rotating facets acts over and above the basic shear strength of the specimen. The higher strain rate does not allow sufficient grain-scale re orientation, resulting in disproportionate distribution in velocity profile - higher

velocity on the lower part of the sample (near the rotating flanges) and nearly zero velocity when moving away from the vicinity of rotating flanges. Concurrently, a radial inertial force, due to the applied higher strain rate may also contribute as a quasi-confining pressure. These phenomena may contribute to the shift in the elastoplastic stiffness response at the high strain rate cases.

The volumetric strain plots Fig. 3(b) show specimen contraction upon progressive shearing – the trend being consistent with previous experimental research [5]. Compared to low confinement, higher confinement promotes greater compression of the specimen. However, a higher strain rate promotes dilative behaviour within the ensemble, which is manifested as delayed contraction when compared to the low strain-rate scenario for the same range of shearing achieved. RR friction also influences the volumetric behaviour, as the samples undergo greater volumetric strain when compared to the idealized specimens – the downward shift in the plot’s attributes to this phenomenon. Idealized specimens are essentially spheres interacting with each other via coulomb friction and as such, cannot resist rotational perturbation upon progressive shearing. RR friction promotes grain-to-grain interlocking, and so higher negative work is done to force a particle scale rearrangement, thus resulting in higher peak strength, prominent volumetric strain and further accompanied by a shift in the residual regime, as observed in the results of Kregel et al. [6].

#### 3.2 Evolution of Porosity and Co-ordination number

The plots of porosity and coordination number (CN) are presented in Fig. 4(a-d) - obtained as an averaged response from discrete RVEs within the specimen



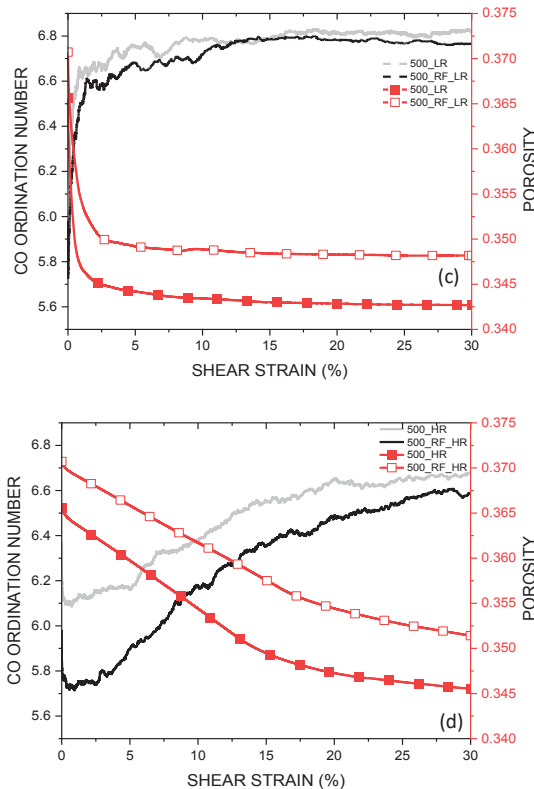


**Figure 4.** Co-ordination number (CN) and Porosity evolution response under 200 and 500 kPa normal stress [Nomenclature: LR/HR – Low rate/High rate; RF-presence of RR friction]

Considering the low strain-rate scenario, the 500 kPa [Fig. 4(c)] confinement promotes a significant reduction in porosity and subsequent increase in CN when compared to 200 kPa confinement [Fig. 4(a)]. Concurrently, compared to idealized specimens, specimens with RR friction show an increased tendency towards attaining higher residual porosity and reduced coordination number upon progressive shearing. However, such response is suppressed at higher confinement, indicating greater particle compression and higher inter-particle contact - as seen from the near overlap of the CN response in Fig. 4 (c). As RR friction mimics angularity, and angular particles promote greater porosity upon progressive shearing, it leads to a loss in inter-particle contact, as observed by Krengel et al. [6]. However, in high strain-rate cases [Fig. 4(b) and (d)], though the general trend of the plots remains similar to a low strain-rate regime, we see a delayed reduction in porosity and slightly higher residual porosity for both confinements. Further, the CN response, as seen in Fig. 4(b) and (d), shows significant reduction when compared with the CN response of low strain-rate samples [Fig. 4(a) and (c)], indicating a significant loss of inter-particle contacts in the residual stage when sheared at high strain rates. This phenomenon is further validated by the higher residual porosity values obtained for the same amount of shearing at high strain rates. The presence of RR friction in specimens imparts angularity, further accentuating

this loss of inter-particle contacts - which is attributed to the concurrent downward shift of CN plots.

## 4 Conclusion

The current study explores the 3D DEM ring shear response of two different monodisperse assemblies of spherical granulates subjected to two-fold constraints – 1) shape (incorporated through rolling resistance (RR) friction parameter) and 2) shear strain rate. Considering both simulation schemes, the increased strain rate accentuates delayed contraction of the specimens. Conversely, higher confinement promotes better contraction along with higher deviatoric strength. A drastic shift in elastoplastic stiffness due to shift in strain rate is noticed. Specimens with particle scale rolling friction give higher peak and residual strength along with increased volumetric strain compared to idealized spherical specimens. Co-ordination number (CN) plots indicate higher inter particle contacts at low strain rate, whereas the high strain response points towards reduced CN response when approaching the residual shearing stage – the reduction accentuates with the presence of RR friction. Porosity evolution plots point towards higher porosity values for specimens with RR friction at the residual stage. However, since the range of strain rates implemented is limited, further micro-scale study is required considering multiple strain rates and simulating realistic particle shapes to substantiate the interdependency of shape and strain rate on bulk behaviour granular material.

## References

1. S.K. Das, A. Das, Influence of quasi-static loading rates on crushable granular materials: A DEM analysis. *Powder Technol.* **344**, 393–403(2019)
2. A. Sadrekarimi, S.M. Olson, Shear band formation observed in ring shear tests on sandy soils. *J. Geotech. Geoenviron. Eng.* **136**, 366–375 (2010).
3. C.M. Wensrich, A. Katterfeld, Rolling friction as a technique for modelling particle shape in DEM. *Powder Technol.* **217**, 409–417 (2012).
4. M. Alam, A. Das, M.M. Disfani, Microstructural behaviour of soft-rigid granular mixes under compressive loads: DEM study using coherent contact model. *Comput. Geotech.* **176**, 106749 (2024).
5. J. Christoffersen, M.M. Mehrabadi, S. Nemat-Nasser, A micromechanical description of granular material behavior. *J. Appl. Mech.* **48**, 339–344 (1981).
6. M.R. Coop, K.K. Sorensen, T. Bodas Freitas, G. Georgoutsos, Particle breakage during shearing of a carbonate sand. *Géotechnique* **54(3)**, 157–163 (2004).
7. D. Krengel, J. Chen, M. Kikumoto, Effects of particle angularity on the bulk-characteristics of granular assemblies under plane strain condition. *Comput. Geotech.* **164**, 105812 (2023).